Brain Ventricular Morphology Analysis Using a Set of Ventricular-Specific Feature Descriptors

Jaeil Kim[1,⋆], Hojin Ryoo[1,⋆], Maria del C. Valdés Hernández[2], Natalie A. Royle[2], and Jinah Park[1,⋆⋆]

[1] Department of Computer Science,
Korea Advanced Institute of Science and Technology,
291 Daehak-ro, Yuseong-gu, Daejeon, Republic of Korea
{threeyears,ryoo.hojin,jinahpark}@kaist.ac.kr
[2] Centre for Clinical Brain Sciences, University of Edinburgh,
Chancellor's Building, 49 Little France Crescent, Edinburgh EH16 4SB, UK
{M.Valdes-Hernan,nat.royle}@ed.ac.uk

Abstract. Morphological changes of the brain lateral ventricles are known to be a marker of brain atrophy. Anatomically, each lateral ventricle has three horns, which extend into the different parts (i.e. frontal, occipital and temporal lobes) of the brain; their deformations can be associated with morphological alterations of the surrounding structures and they are revealed as complex patterns of their shape variations across subjects. In this paper, we propose a novel approach for the ventricular morphometry using structural feature descriptors, defined on the 3D shape model of the lateral ventricles, to characterize its shape, namely width, length and bending of individual horns and relative orientations between horns. We also demonstrate the descriptive ability of our feature-based morphometry through statistical analyses on a clinical dataset from a study of aging.

1 Introduction

The brain lateral ventricles are cavities filled by cerebrospinal fluid (CSF) limited by an epithelial membrane called ependymal. The morphological deformations on the lateral ventricles have been related to neurodegenerative diseases [7] and cognitive decline [2]. It has also been reported that the ventricular volume and width may be predictors to determine the quality of brain surgical treatments, such as deep brain stimulation surgery [4] and ventricular catheter placement [20].

Deformations of the lateral ventricles have been investigated through various approaches that involve assessing the volume [3], ventricular surface [13] and medial thickness [10]. However, the analysis of the ventricular deformations is still

⋆ Both authors contributed equally to this work.
⋆⋆ Corresponding author.

F. Bello and S. Cotin (Eds.): ISBMS 2014, LNCS 8789, pp. 141–149, 2014.

challenging. Since the lateral ventricles are essentially a brain cavity with irregular shape, its shape changes can be atypical and revealed as complex patterns across subjects. This not only applies to each horn individually, but also to the "C-shape" that curves from the temporal horn into the beginning of the frontal horn [18], which also varies across subjects. The atrium of the lateral ventricles is the place where the three horns meet, and it can also change depending on each horn's enlargement and on changes in the shape of the surrounding structures. Due to the adaptive capacity of the ventricular system filled by CSF, its structural changes may be related to the alteration of the surrounding parenchymal structures [13]. Therefore decomposing the structural changes of the lateral ventricle anatomically can lead to a better understanding of the ventricular deformations in relation to the surrounding structures.

For the morphology analysis of the brain ventricles, several indices quantifying the structural characteristics of the ventricles have been proposed. With respect to the interior and exterior of the lateral ventricles, these shape indices of the ventricles can reveal the atrophy of the interior structures of the medial temporal lobe or the global and lobar atrophy of the brain [8]. For instance, the radial width of the temporal horn was introduced to measure the enlargement of the temporal horn [8] and to investigate the atrophy of the hippocampus where the memory consolidates [5]. Some clinical studies reported that the atrophy of the frontal lobe is related with aging and cognitive decline [2,5], diabetes and drug addiction [13,15]. To trace the enlargement of the frontal horn of the lateral ventricle, the structural measures, such as ventricular angle and frontal horn radius, has been used [4,17] as well as 3D shape models of the ventricle. These structural indices can provide a straightforward description of the ventricular shape and its changes. However, the manual measurement of them makes it susceptible to human errors and imaging protocols.

By providing an automated modeling strategy that consistently characterizes the shape of the lateral ventricle across subjects, we are addressing the needs on computational analyses: intuitive shape description and reproducibility. Based on the surface mesh of the lateral ventricle, we propose a set of the explicit feature descriptors as a pre-defined layout of its shape description to quantify the structural characteristics (e.g. horn length, radius and bending) independently. We propose two types of feature descriptors: (1) individual features for quantifying the shape and size of each horn, and (2) inter-horn features for characterizing the C-shape and the atrium of the lateral ventricles. We also demonstrate the descriptive ability of our feature-based morphometry through the statistical analysis on a dataset from a study of aging.

2 Ventricular Shape Representation

We model the shape of lateral ventricles as a smooth surface mesh and its central skeleton. These model components form the basis of our approach allowing quantifying the structural characteristics of the individual horns and between the horns.

First of all, the surface mesh of lateral ventricle is constructed from binary masks, obtained from brain MR images, via a template-based surface modeling approach [14]. We construct a template mesh of the lateral ventricle using an average shape image, generated from the binary masks via a image registration based approach [12]. We optimally align the template mesh to each binary mask and propagate it to the image boundary while minimizing the distortion of its point distribution against arbitrary size variations. This method builds a pairwise correspondence between the template of average shape and the targets of each subject.

On the reconstructed meshes, we easily determine the tips of the individual horns, owing to the point correspondence with the template. They are used for the construction of the skeleton. For the skeleton construction, we use a Voronoi diagram-based approach where the centers of the maximal inscribed spheres (MIS) are defined within and along the surface mesh [1]. We used the vascular modeling toolkit (VMTK, Ver. 1.2) for this process. Technically, from two terminal points and the surface model, the skeleton is constructed by finding a path between two points, which minimizes the integral of the inverse radius of the MIS on the Voronoi diagram of the surface model [19].

In the ventricular shape representation, the most important structure is the central skeleton which consists of the atrium center and the horn skeleton (See Figure 1). The *atrium center* is defined as a center of the ventricular atrium region. To determine the atrium center, we first compute three tip-to-tip skeletons; the frontal-temporal, the temporal-occipital, and the occipital-frontal skeleton. Then, the atrium center is computed by finding an optimal position which has equal minimum distance to the three tip-to-tip skeletons on the Voronoi diagram. The atrium center is assigned to be a common terminal point for constructing the skeletons of the three horns, which are referred each as "(frontal/temporal/occipital) horn skeleton". The horn skeleton is the skeleton connecting the atrium center and the tips of each horn.

Other feature landmarks necessary to determine the domain of the feature measurement characterizing each horn's morphology are the *starting and ending points* for each horn-skeleton. The starting point is determined by the center of the MIS that passes through the atrium center in the horn skeleton, and the ending point is the center of the last MIS passing through the tip of each horn. We also define two vectors for each horn – *starting and ending vectors* – from the atrium center to the starting and ending points, respectively.

3 Structural Feature Descriptors for the Lateral Ventricle

On the representation model of the lateral ventricle, we define the two types of feature descriptors, the individual horn descriptors and the inter-horn descriptors, which quantify the geometric characteristics for the lateral ventricle.

As individual horn structural descriptors, we define the width, length, and bending of each horn with respect to its skeleton. The *width* descriptor informs how large the cross-section of the horn is. Once we determine the closest distance from each vertex of the surface mesh to the skeleton, we calculate the width at

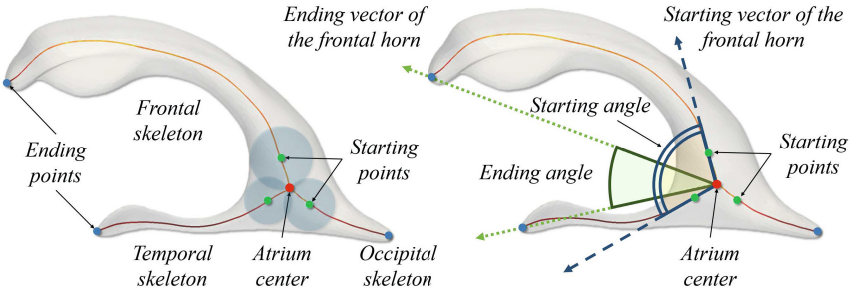

Fig. 1. Ventricular shape model with its skeleton and landmarks. The green and blue points indicate respectively the starting and ending point of each horn skeleton, and the red point indicates the atrium center. The starting vectors (dotted arrow) and the ending vectors (dashed arrow) are referred to measure the angles between two horns.

each sampled point of the skeleton as the average of the closest distance to the vertices of the surface mesh, which are nearest to the sampled points. The skeleton is segmented at a regular interval of a unit distance to determine the sampled points. We use the average value of the width at each sampled point and the width at the starting point as ventricular feature descriptors. The *length* of each horn refers to the geodesic length of the skeleton, which is calculated by summing the Euclidean distances between the sampled points of the skeleton. The *bending* of each horn is estimated as the ratio of the geodesic length to the Euclidean distance between the starting and ending points for each horn.

As inter-horn structural descriptors, we define the width at the atrium center and the angles representing the relative orientations between horns and the C-shape of the lateral ventricle. Since the three skeletons encounter each other at the atrium center, the *atrium width* is estimated by averaging the width at the atrium center for the three horn skeletons. We define a pair of angle measures – *starting and ending angles* – with respect to two neighboring horns. The starting and ending angles are the angles between the starting and ending vectors of two horns, respectively. The starting angle estimates the degree of the relative orientations of each horn nearby the atrium, and the ending angle quantifies the angle between the tip of the horns with respect to the atrium center.

4 Morphology Analysis Using the Feature Descriptors

In order to assess the descriptive ability of the feature descriptors, we performed two analyses on a dataset of a study of aging: (1) a feature-based description of the shape variations of the lateral ventricle within a population, and (2) a ventricular enlargement analysis using the feature descriptors in relation to general brain atrophy. Without loss of generality, we present the experiment results of the left lateral ventricle only. The morphology of the right lateral ventricle can be quantified in the same way.

The dataset includes T1-weighted MR images obtained at a GE Signa HDxt 1.5T scanner, (General Electric, USA) from 33 participants (10 women and 23 men, age = 72.7 ± 0.7 years) randomly selected from The Lothian Birth Cohort 1936 study [6]. The scanning protocol is described in detail elsewhere [21]. The dataset also contains the brain tissue volume (BTV) and intracranial volume, and the binary masks of the lateral ventricles, following the segmentation procedure described in [3]. The results were visually assessed by a trained image analyst and manually corrected. From these binary ventricular masks we obtained the surface models as described previously. We validated the accuracy of this process using the Dice coefficient and the symmetric mean distance between the models and the target volumes. The reconstructed models showed high accuracy with the segmentations: Dice coefficient was 0.954 ± 0.013, and the mean distance was 0.642 ± 0.763 mm for all subjects.

4.1 Feature-Based Description of Shape Variations across all Subjects

In order to investigate the shape variations of the lateral ventricles across the sample, we first computed the mean surface shape and its deviations using principal component analysis (PCA) and transformed them into the feature space. For the PCA, we normalized the surface models via isotropic rescaling using the intracranial volume, and aligned them optimally by matching the atrium center and rotating each of them to minimize the between-surface distance via a Procrustes analysis [9]. The mean surface model was computed simply by averaging the corresponding points on the surface models: $\bar{x} = \sum_{i=1}^{n} x_i$, where x_i is a $3 \times k$ vector describing the surface model with k points and n is the number of subjects. The covariance matrix is given by: $D = \frac{1}{n-1} \sum_{i=1}^{n} (x_i - \bar{x}) \cdot (x_i - \bar{x})^T$. The eigen-decomposition on D delivers the $\min(n-1, 3k)$ principal modes of the variation [11]. A mode with a high variance (i.e. large eigenvalue of D) represents a larger part of the shape variation of the lateral ventricle across subjects. The percentage of the shape variability of each mode is determined by the ratio between the corresponding eigenvalue and the sum of the eigenvalues [16]. We generated the surface models showing the shape variations of each mode between ± 3 standard deviations (SD) and extracted the feature descriptors from them.

Figure 2 shows the surface meshes of the largest and smallest size with the average surface mesh and the surface models representing the shape variation of the first and second modes between ± 3 SD with their skeletons. The percentage of the shape variability of the first mode was 50.75 % in this population, and the second mode was 13.62 %. The shape variability of each mode can be explained more intuitively using the feature descriptors. For example, the visual observation of the morphological variation along the 'frontal horn' of ± 3 SD of the first mode in Figure 2 can be described based on the measured values of feature descriptors (Table 1) as follows: the average width, starting width, and the geodesic length of the frontal horn decreased, while the bending increased from the -3 to the +3 SD. Moreover, the morphological relationship between two

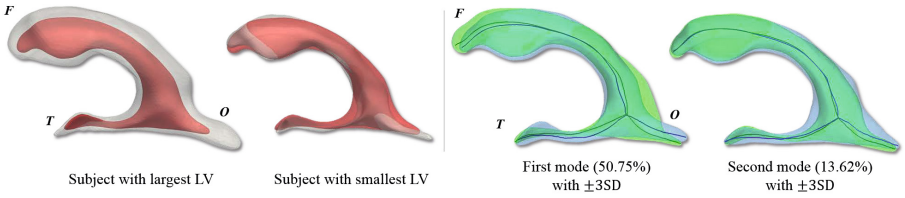

Fig. 2. (Left) ventricular surface meshes (white) of the largest and smallest size with the average surface mesh (red). (Right) Surface meshes with their skeletons representing the shape variation of the first and second modes between ± 3 standard deviations (SD). The surface, skeleton and bars on blue color correspond to + 3 SD, and those on green color to – 3 SD. F: frontal horn, T: temporal horn and O: occipital horn.

horns is expressed by the inter-horn feature descriptors. For instance, the bending of the temporal and occipital horns highly increased towards the -3 SD. On the other hand, the start and ending angles between these two horns increased on the +3 SD surface model, which reflected the two horns were widely opened than -3 SD. Therefore, analyzing both sets of feature descriptors together we can interpret that the temporal and occipital horn are bending to each other when ventricular shapes differ from the mean going from +3 to -3 SD of the first mode. Observe on Figure 2 that the other values of the feature descriptors were also reflecting consistently the shape differences between the surface models of ± 3 SD of the first mode.

Table 1. Measure values of the feature descriptors on the surface meshes of ± 3 SD of the first mode

Individual-horn Feature Descriptors												
	Frontal Horn				Temporal Horn				Occipital Horn			
	MW	SW	GL	Bend	MW	SW	GL	Bend	MW	SW	GL	Bend
+3SD	4.71	5.16	90.43	0.20	1.50	4.60	51.89	0.13	2.55	5.18	23.01	0.05
Avg	4.67	4.28	89.24	0.21	1.77	4.18	50.67	0.11	2.23	4.74	22.42	0.03
-3SD	4.65	4.29	88.56	0.22	2.00	4.47	49.29	0.10	2.39	4.00	22.86	0.02

Inter-horn Feature Descriptors							
	AW	SA (FT)	SA (TO)	SA (OF)	EA (FT)	EA (TO)	EA (OF)
+3SD	6.11	108.19	102.10	149.22	33.05	133.80	200.13
Avg	5.92	102.78	112.43	144.65	32.88	137.83	198.67
-3SD	5.59	112.61	120.92	126.13	33.08	143.81	162.52

MW.: mean width (mm), SW.: starting width (mm), GL.: geodesic length (mm), Bend.: bending, AW.: atrium width (mm), SA.: starting angle (°), EA.: ending angle (°), FT.:frontal-temporal, TO.: temporal-occipital, and OF.: occipital-frontal

±3SD: surface mesh corresponding to ±3 SD of the first mode, and Avg.: average surface mesh

4.2 A Morphological Feature Analysis with a General Brain Atrophy Measure

It is known that cerebral atrophy is a common accompaniment of aging and manifests as decreased total brain volume and increased ventricular volumes [3]. In order to evaluate the descriptive ability of the feature descriptors in relation to brain atrophy, we examined the associations between each feature descriptor and brain tissue volume (BTV). For this we performed a robust multilinear regression using the function "robustfit" from MATLAB Statistical Toolbox. The regression model includes the feature descriptors as the dependent variable and BTV as the independent variable, with gender and age as covariates.

The regression analysis showed that the average width of each horn was increased as the BTV decreased (β = -8.197 $\sim$ -10.470, P $<$ 0.05). The width of the atrium also increased as the BTV decreased (β = -20.652, P $<$ 0.05). Near the atrium of the lateral ventricle, the width of the frontal and occipital horns were not significantly associated with brain atrophy (P $>$ 0.05), but it was for the temporal horn (β = -17.791, P $<$ 0.05). The geodesic length and bending of each horn were not significantly related to brain atrophy and the angular measurements between horns with respect to the atrium center were not associated to the brain atrophy either. These results indicate that the association between ventricular enlargement and general brain atrophy is manifested as the significant increase of the width along the ventricular central axes (i.e. skeleton) despite of the complex patterns of shape variations observed in this population sample through PCA.

Table 2. Association between a brain atrophy measure (brain tissue volume) and the feature descriptors of the lateral ventricle using a robust multilinear regression (beta, P).

Linear Regression on Individual Horn Structural Feature Descriptors				
	Mean Width	Starting Width	Geodesic Length	Bending
Frontal Skeleton	**-10.470, 0.011**	-12.552, 0.100	28.109, 0.328	0.283, 0.068
Temporal Skeleton	**-8.197, 0.002**	**-17.791, 0.003**	-4.239, 0.849	-0.043, 0.820
Occipital Skeleton	**-8.763, 0.039**	-9.820, 0.104	-60.131, 0.370	0.165, 0.132

Linear Regression on Inter-horn Structural Feature Descriptors		
Atrium Width	**-20.652, 0.035**	
	Angle between Starting Points with Atrium Center	Angle between Ending Points with Atrium Center
Frontal-Temporal	18.224, 0.749	-21.239, 0.159
Temporal-Occipital	-11.750, 0.826	23.766, 0.501
Occipital-Frontal	-22.718, 0.603	-18.809, 0.871

Regression Model: Structural Feature (Enlargement) = β_1* Brain Tissue Volume/Intracranial Volume + β_2 * Gender + β_3 * age
beta, P : Unstandardized coefficients and P-values of the regression models
Significant values (P $<$ 0.05) are highlighted as boldface

5 Conclusion

In this paper, we introduce a set of descriptors, that characterize the lateral ventricle's morphology, with an explicit measurement basis that includes the definitions of the ventricular skeleton and atrium center on the shape model. We demonstrate through statistical analyses on 33 randomly selected datasets from a study of aging how the feature descriptors can express the changes of the lateral ventricle with respect to the general brain atrophy. We also present the descriptive ability of the feature descriptors using PCA-based shape models representing the shape variations across subjects. The structural feature descriptors can provide a precise description of the ventricular shapes based on anatomical knowledge for the morphology analysis of the lateral ventricle. We anticipate that these shape feature descriptors of the lateral ventricle would be useful in characterizing its deformation more systematically. Further work is needed to investigate the relationships between each feature descriptor and the role they play in the volumetric changes observed on the lateral ventricles. In addition, the application to larger samples is also needed to generalize the sensitivity of the feature descriptors and to validate the consistency of the anatomical landmarks (e.g. tips of the ventricular horns) across subjects.

Acknowledgments. This work was funded by the National Research Foundation of Korea (Grant no. 2012K2A1A2033133/no.2011-0009761), the Row Fogo Charitable Trust, the Scottish Imaging Network A Platform for Scientific Excellence and Age UK for the LBC1936 Study. We also thank the Lothian Birth Cohort 1936 Study Collaborative Group at The University of Edinburgh led by Profs. Ian J. Deary and Joanna M. Wardlaw, who provided the data used in this manuscript.

References

1. Antiga, L., Ene-Iordache, B., Remuzzi, A.: Computational geometry for patient-specific reconstruction and meshing of blood vessels from MR and CT angiography. IEEE Trans. Med. Imaging 22(5), 674–684 (2003)
2. Apostolova, L.G., Green, A.E., Babakchanian, S., Hwang, K.S., Chou, Y.Y., Toga, A.W., Thompson, P.M.: Hippocampal atrophy and ventricular enlargement in normal aging, mild cognitive impairment (MCI), and Alzheimer Disease. Alz. Dis. Assoc. Dis. 26(1), 17–27 (2012)
3. Aribisala, B.S., Valdés Hernández, M.C., Royle, N.A., Morris, Z., Muñoz Maniega, S., Bastin, M.E., Deary, I.J., Wardlaw, J.M.: Brain atrophy associations with white matter lesions in the ageing brain: the Lothian Birth Cohort 1936. Eur. Radiol. 23(4), 1084–1092 (2013)
4. Bourne, S.K., Conrad, A., Konrad, P.E., Neimat, J.S., Davis, T.L.: Ventricular width and complicated recovery following deep brain stimulation surgery. Stereotact Funct. Neurosurg. 90(3), 167–172 (2012)
5. Buckner, R.L.: Memory and executive function in aging and ad: multiple factors that cause decline and reserve factors that compensate. Neuron 44(1), 195–208 (2004)

6. Deary, I.J., Gow, A.J., Taylor, M.D., Corley, J., Brett, C., Wilson, V., Campbell, H., Whalley, L.J., Visscher, P.M., Porteous, D.J., Starr, J.M.: The Lothian Birth Cohort 1936: a study to examine influences on cognitive ageing from age 11 to age 70 and beyond. BMC Geriatr. 7, 28 (2007)
7. Ferrarini, L., Palm, W.M., Olofsen, H., van Buchem, M.A., Reiber, J.H.C., Admiraal-Behloul, F.: Shape differences of the brain ventricles in Alzheimer's disease. NeuroImage 32(3), 1060–1069 (2006)
8. Frisoni, G.B., Geroldi, C., Beltramello, A., Bianchetti, A., Binetti, G., Bordiga, G., DeCarli, C., Laakso, M.P., Soininen, H., Testa, C., et al.: Radial width of the temporal horn: a sensitive measure in alzheimer disease. American Journal of Neuroradiology 23(1), 35–47 (2002)
9. Gower, J.C.: Generalized procrustes analysis. Psychometrika 40(1), 33–51 (1975)
10. Gutman, B.A., Wang, Y., Rajagopalan, P., Toga, A.W., Thompson, P.M.: Shape matching with medial curves and 1-D group-wise registration. In: 2012 9th IEEE International Symposium on Biomedical Imaging, pp. 716–719 (2012)
11. Heimann, T., Meinzer, H.P.: Statistical shape models for 3D medical image segmentation: A review. Med. Image Anal. 13(4), 543–563 (2009)
12. Heitz, G., Rohlfing, T., Maurer, J.C.R.: Statistical shape model generation using nonrigid deformation of a template mesh. In: SPIE on Medical Imaging, pp. 1411–1421 (2005)
13. Jeong, H.S., Lee, S., Yoon, S., Jung, J.J., Cho, H.B., Kim, B.N., Ma, J., Ko, E., Im, J.J., Ban, S., Renshaw, P.F., Lyoo, I.K.: Morphometric abnormalities of the lateral ventricles in methamphetamine-dependent subjects. Drug Alcohol Depend 131(3), 222–229 (2013)
14. Kim, J., Park, J.: Organ Shape Modeling Based on the Laplacian Deformation Framework for Surface-Based Morphometry Studies. J. Comp. Sci. Eng. 6, 219–226 (2012)
15. Lee, J.H., Yoon, S., Renshaw, P.F., Kim, T.S., Jung, J.J., Choi, Y., Kim, B.N., Jacobson, A.M., Lyoo, I.K.: Morphometric changes in lateral ventricles of patients with recent-onset type 2 diabetes mellitus. PloS One 8(4), e60515 (2013)
16. Lu, Y.C., Untaroiu, C.D.: Statistical shape analysis of clavicular cortical bone with applications to the development of mean and boundary shape models. Comput. Meth. Prog. Bio. 111(3), 613–628 (2013)
17. Ng, H.-F., Chuang, C.-H., Hsu, C.-H.: Extraction and Analysis of Structural Features of Lateral Ventricle in Brain Medical Images. In: 2012 Sixth International Conference on Genetic and Evolutionary Computing (ICGEC), pp. 35–38 (2012)
18. Nolte, J.: Essentials of the Human Brain. Elsevier Health Sciences (2009)
19. Piccinelli, M., Veneziani, A., Steinman, D.A., Remuzzi, A., Antiga, L.: A framework for geometric analysis of vascular structures: application to cerebral aneurysms. IEEE Trans. Med. Imaging 28(8), 1141–1155 (2009)
20. Wan, K.R., Toy, J.A., Wolfe, R., Danks, A.: Factors affecting the accuracy of ventricular catheter placement. J. Clin. Neurosci. 18(4), 485–488 (2011)
21. Wardlaw, J.M., Bastin, M.E., Valdés Hernández, M.C., Maniega, S.M., Royle, N.A., Morris, Z., Clayden, J.D., Sandeman, E.M., Eadie, E., Murray, C., Starr, J.M., Deary, I.J.: Brain aging, cognition in youth and old age and vascular disease in the Lothian Birth Cohort 1936: rationale, design and methodology of the imaging protocol. Int. J. Stroke 6(6), 547–559 (2011)